

# Interaction of $\pi$ -Conjugated Organic Molecules with $\pi$ -Bonded Semiconductor Surfaces: Structure, Selectivity, and Mechanistic Implications

Michael P. Schwartz, Mark D. Ellison,<sup>†</sup> Sarah K. Coulter, Jennifer S. Hovis,<sup>‡</sup> and Robert J. Hamers\*

Contribution from the Department of Chemistry, University of Wisconsin-Madison, 1101 University Avenue, Madison, Wisconsin 53706

Received March 15, 2000

**Abstract:** The (001) surface of silicon contains pairs of atoms that are held together with a strong  $\sigma$  bond and a weak  $\pi$  bond. The interaction of styrene with the Si(001) surface has been investigated as a model system for understanding the interaction of conjugated  $\pi$ -electron systems to  $\pi$ -bonded semiconductor surfaces. Scanning tunneling microscopy images show one primary bonding configuration, slightly off-center from the middle of a dimer row. Infrared spectra using isotopically labeled styrene establish that attachment occurs in a highly selective way, bonding through the external vinyl group and leaving the aromatic ring almost completely unperturbed. Ab initio calculations reveal that the interaction between the  $\pi$  electrons of the vinyl group of styrene and the electron-deficient end of a Si=Si dimer is strongly attractive. It is proposed that this attraction facilitates a low-symmetry interaction between the surface dimers and the vinyl group, leading to a highly selective reaction pathway for which Woodward–Hoffmann rules do not apply. The implications for selective attachment of other conjugated  $\pi$ -electron systems to other  $\pi$ -bonded semiconductor surfaces are discussed.

## I. Introduction

Recent studies have shown that there are some strong analogies that can be drawn linking the chemistry of the (001) surfaces of Si, Ge, and C(diamond) with the chemistry of disilenes (compounds with Si=Si double bonds) and alkenes. In particular, these studies have shown that various types of “cycloaddition” reactions, widely used in organic chemistry to form ring systems, can be applied to link organic molecules to the (001) surfaces of silicon,<sup>1–20</sup> germanium,<sup>21–23</sup> and diamond.<sup>24,25</sup> In some cases these reactions form monolayers of molecules that are ordered and oriented along specific crystal-

lographic directions.<sup>4,5,26,27</sup> In addition to being a rich area of scientific interest, the development of general strategies for fabrication of well-defined interfaces between silicon and organic materials is expected to play an important role in new and emerging technology areas such as molecular electronics and biotechnology. Attachment of organic molecules containing delocalized  $\pi$ -electron systems is of especially keen interest because larger oligomers and polymers are known to be semiconductors or metals.<sup>28</sup> To retain these interesting electrical properties after attachment to a surface, however, the attachment process must not adversely modify the electronic structure of

\* Address correspondence to this author. E-mail: rjhamers@facstaff.wisc.edu.

<sup>†</sup> Present Address: Department of Chemistry, Wittenberg University, Springfield, OH 45501.

<sup>‡</sup> Present Address: Department of Chemistry, Stanford University, Stanford, CA 94305.

(1) Yoshinobu, J.; Tsuda, H.; Onchi, M.; Nishijima, M. *J. Chem. Phys.* **1987**, *87*, 7332.

(2) Bozack, M. J.; Taylor, P. A.; Choyke, W. J.; Yates, J. T., Jr. *Surf. Sci.* **1986**, *177*, L933–L937.

(3) Clemen, L.; Wallace, R. M.; Taylor, P. A.; Dresser, M. J.; Choyke, W. J.; Weinberg, W. H.; Yates, J. T., Jr. *Surf. Sci.* **1992**, *268*, 205–216.

(4) Hamers, R. J.; Hovis, J.; Lee, S.; Liu, H.; Shan, J. *J. Phys. Chem.* **1997**, *101*, 1489–1492.

(5) Hovis, J. S.; Hamers, R. J. *J. Phys. Chem., B* **1998**, *102*, 687–692.

(6) Hovis, J. S.; Liu, H. B.; Hamers, R. J. *J. Phys. Chem., B* **1998**, *102*, 6873–6879.

(7) Konecny, R.; Doren, D. *J. Surf. Sci.* **1998**, *417*, 169–188.

(8) Teplyakov, A. V.; Kong, M. J.; Bent, S. F. *J. Am. Chem. Soc.* **1997**, *119*, 11100–11101.

(9) Teplyakov, A. V.; Kong, M. J.; Bent, S. F. *J. Chem. Phys.* **1998**, *108*, 4599–4606.

(10) Cheng, C. C.; Wallace, R. M.; Taylor, P. A.; Choyke, W. J.; Yates, J. T. *J. Appl. Phys.* **1990**, *67*, 3693–3699.

(11) Mayne, A. J.; Avery, A. R.; Knall, J.; Jones, T. S.; Briggs, G. A. D.; Weinberg, W. H. *Surf. Sci.* **1993**, *284*, 247–256.

(12) Imamura, Y.; Morikawa, Y.; Yamasaki, T.; Nakatsuji, H. *Surf. Sci.* **1995**, *341*, L1091.

(13) Liu, Q.; Hoffman, R. *J. Am. Chem. Soc.* **1995**, *117*, 4082.

(14) Mayne, A. J.; Cataldi, T. R. I.; Knall, J.; Avery, A. R.; Jones, T. S.; Pinheiro, L.; Hill, H. A. O.; Briggs, G. A. D.; Pethica, J. B.; Weinberg, W. H. *Faraday Discuss. R. Soc.* **1992**, *94*, 199.

(15) Taylor, P. A.; Wallace, R. M.; Cheng, C. C.; Weinberg, W. H.; Dresser, M. J.; Choyke, W. J.; Yates, J. T., Jr. *J. Am. Chem. Soc.* **1992**, *114*, 6754.

(16) Widdra, W.; Huang, C.; Yi, S. I.; Weinberg, W. H. *J. Chem. Phys.* **1996**, *105*, 5605–5617.

(17) Liu, H.; Hamers, R. J. *J. Am. Chem. Soc.* **1997**, *119*, 7593–7594.

(18) Huang, C.; Widdra, W.; Wang, X. S.; Weinberg, W. H. *J. Vac. Sci. Technol. A* **1993**, *11*, 2250–2254.

(19) Huang, C.; Widdra, W.; Weinberg, W. H. *Surf. Sci.* **1994**, *315*, L953.

(20) Craig, B. I. *Surf. Sci.* **1995**, *329*, 293–294.

(21) Lee, S. W.; Nelen, L. N.; Ihm, N.; Scoggins, T.; Greenlief, C. M. *Surf. Sci.* **1998**, *410*, L773–L778.

(22) Hamers, R. J.; Hovis, J. S.; Greenlief, C. M.; Padowitz, D. F. *Jpn. J. Appl. Phys., Part 1* **1999**, *38*, 3879–3887.

(23) Lee, S. W.; Hovis, J. S.; Coulter, S. K.; Hamers, R. J.; Greenlief, C. M. *Surf. Sci.* Accepted for publication.

(24) Hovis, J. S.; Coulter, S. K.; Hamers, R. J.; D'Evelyn, M. P.; Russell, J. N.; J. E., B. *J. Am. Chem. Soc.* **2000**, *122*, 732–733.

(25) Wang, G. T.; Bent, S. F.; Russell, J. N., Jr.; Butler, J. E.; D'Evelyn, M. P. *J. Am. Chem. Soc.* **2000**, *122*, 744–745.

(26) Hovis, J. S.; Hamers, R. J. *J. Phys. Chem. B* **1997**, *101*, 9581–9585.

(27) Hovis, J. S.; Liu, H.; Hamers, R. J. *Surf. Sci.* **1998**, *402–404*, 1–7.

(28) Reddinger, J. L.; Reynolds, J. R. *Adv. Polym. Sci.* **1999**, *145*, 57–122.

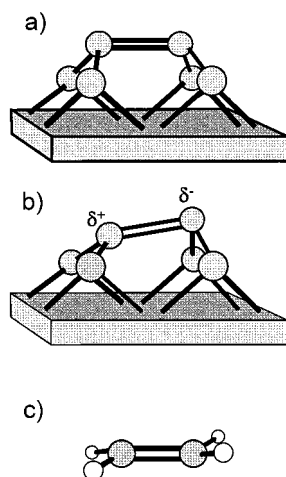


**Figure 1.** Schematic illustrations of moieties containing Si=Si double bonds: (a) symmetric Si=Si dimer of the Si(001) surface; (b) tilted Si=Si dimer of the Si(001) surface; and (c) disilene shown in the equilibrium trans configuration.

the  $\pi$ -conjugated system. Consequently, there is great motivation to understand the factors controlling selectivity in the interactions of more complex molecules with silicon surfaces.

Si(001), Ge(001), and C(001) surfaces all undergo a similar surface reconstruction in which adjacent atoms pair together into dimers, as shown in Figure 1a. The bonding between the atoms can be described in terms of a strong  $\sigma$  bond and a weaker  $\pi$  bond,<sup>29–31</sup> making them structurally and electronically similar to the Si=Si bonds of disilenes<sup>32,33</sup> and the C=C bonds of alkenes. Compared with the familiar planar configuration of alkenes, however, the  $\pi$ -bonded dimers at the Si(001) surface have two types of distortion. The first distortion arises from the fact that, as shown in Figure 1a, the bonds between the surface Si atoms and the underlying bulk are not coplanar. This distortion weakens the Si=Si  $\pi$  bond and makes the ends of the dimer more accessible to impinging reactant molecules. The second distortion is tilting of the dimer units out of the surface plane (Figure 1b), which leads to transfer of electron density from the “down” to the “up” atom.<sup>34</sup> Similar distortions occur spontaneously for many disilenes (compounds containing Si=Si double bonds), such as the molecule disilene, Si<sub>2</sub>H<sub>4</sub>, depicted in Figure 1c.<sup>35</sup> In fact, the high reactivity of the Si=Si groups in disilenes has been attributed largely to the fact that the bond-angle deformations involve rather low energies, leading to a greater propensity to react through low-symmetry and/or diradical mechanisms.<sup>36</sup> Similarly, the high reactivity of the Si(001) surface can be attributed in part to the nonplanar nature of the bonds between the Si=Si dimer and the underlying bulk substrate.

The similarities in structure between the  $\pi$ -bonded dimers on these dimerized semiconductor surfaces and the more conventional double bonds of disilenes and alkenes leads to a strong motivation to understand whether there are analogous

similarities in their *chemistry*. A number of recent studies have focused on cycloaddition reactions between organic molecules and dimerized surfaces of Si, Ge, and diamond. The adsorption of an alkene onto the Si(001) surface can be viewed as utilizing two electrons from the  $\pi$ -bond of one Si=Si dimer and two electrons from the  $\pi$ -bond of the alkene to form two new strong Si–C bonds.<sup>1,17–20</sup> This reaction is formally equivalent to a [2+2] cycloaddition reaction. Recent studies have shown that while the reaction of two simple alkenes via a high-symmetry suprafacial–suprafacial pathway is symmetry-forbidden,<sup>37</sup> reactions producing [2+2]-like products on Si(001),<sup>2,4</sup> Ge(001),<sup>22,38</sup> and, to a lesser extent, the diamond(001)<sup>24</sup> surface are surprisingly facile. This implies that the “[2+2]” reactions on Si(001) are not truly concerted reactions, and that they instead proceed via a low-symmetry intermediate for which the orbital symmetry rules do not apply.<sup>6,24,39</sup>

The facile nature of [2+2] reactions on these surfaces has important implications for controlling selectivity in more complex systems. For example, molecules with two conjugated C=C bonds can react with the dimerized (001) surfaces of Si,<sup>6,8,9</sup> Ge,<sup>21</sup> and diamond<sup>25</sup> via the equivalent of a [4+2] (Diels–Alder) reaction. However, interaction via a [2+2] process using only one C=C bond also occurs, leading to a mix of [2+2] and [4+2] products.<sup>6,39,40</sup> Even though the [4+2] product is predicted to be more stable, the high strength of the Si–C bond causes the product distribution to be controlled by the initial dynamics of the molecule–surface interaction, rather than the thermodynamics of the final product.<sup>6,39</sup>

While for simple alkenes and conjugated dienes the initial molecule–surface dynamics combined with the high Si–C bond strength locks in a kinetically controlled distribution of products, there is some evidence that aromatic systems may be an important exception. Recent studies have shown that benzene<sup>22,41–45</sup> and toluene<sup>45</sup> can undergo (irreversible) changes in bonding configuration at room temperature. Furthermore, at elevated temperatures benzene desorbs from the surface without fragmentation.<sup>41,42</sup> The ability of benzene and toluene to undergo transitions from one configuration to another suggests that the aromaticity of the free molecules leads to surface adducts that are comparatively weakly bound. The decreased stability of the adducts might be expected to be accompanied by a reduced activation barrier for diffusion, and an increased propensity toward forming the thermodynamically favored product.

To understand selectivity in bonding of molecules to surfaces, it is imperative to understand under what conditions product distributions are controlled by dynamics, and when they are controlled by thermodynamics. In this paper, we report investigations using styrene as a model system for understanding the chemical and structural factors that control the bonding of  $\pi$ -conjugated molecules to  $\pi$ -bonded semiconductor surfaces.

(37) Woodward, R. B.; Hoffmann, R. *The Conservation of Orbital Symmetry*; Academia Press: New York, 1970.

(38) Lal, P.; Teplyakov, A. V.; Noah, Y.; Kong, M. J.; Wang, G. T.; Bent, S. F. *J. Chem. Phys.* **1999**, *110*, 10545–10553.

(39) Choi, C. H.; Gordon, M. S. *J. Am. Chem. Soc.* **1999**, *121*, 11311–11317.

(40) Wang, G. T.; Mui, C.; Musgrave, C. B.; Bent, S. F. *J. Phys. Chem. B* **1999**, *103*, 6803–6808.

(41) Lopinski, G. P.; Fortier, T. M.; Moffatt, D. J.; Wolkow, R. A. *J. Vac. Sci. Technol., A* **1998**, *16*, 1037–1042.

(42) Lopinski, G. P.; Moffatt, D. J.; Wolkow, R. A. *Chem. Phys. Lett.* **1998**, *282*, 305–312.

(43) Kong, M. J.; Teplyakov, A. V.; Lyubovitsky, J. G.; Bent, S. F. *Surf. Sci.* **1998**, *411*, 286–293.

(44) Taguchi, Y.; Fujisawa, M.; Takaoka, T.; Okada, T.; Nishijima, M. *J. Chem. Phys.* **1991**, *95*, 6870–6876.

(45) Coulter, S. K.; Hovis, J. S.; Ellison, M. D.; Hamers, R. J. *J. Vac. Sci. Technol.* **2000**, *A18*, 1965.

(29) Appelbaum, J. A.; Baraff, G. A.; Hamann, D. R. *Phys. Rev. B* **1976**, *14*, 588.

(30) Hamers, R. J.; Tromp, R. M.; Demuth, J. E. *Phys. Rev. B* **1986**, *34*, 5343–5357.

(31) Hamers, R. J.; Tromp, R. M.; Demuth, J. E. *Surf. Sci.* **1987**, *181*, 246–355.

(32) Dixon, C. E.; Liu, H. W.; VanderKant, C. M.; Baines, K. M. *Organometallics* **1996**, *15*, 5701–5705.

(33) Dixon, C. E.; Baines, K. M. *Phosphorus, Sulfur, Silicon* **1997**, *124–125*, 123–132.

(34) Chadi, D. J. *Phys. Rev. Lett.* **1979**, *43*, 43–47.

(35) Karni, M.; Apeloig, Y. *J. Am. Chem. Soc.* **1990**, *112*, 8589–8590.

(36) Liang, C.; Allen, L. *J. Am. Chem. Soc.* **1990**, *112*, 1039–1041.

Our results show that styrene exhibits a high degree of selectivity in bonding to Si(001), bonding almost exclusively through the vinyl group. Contrary to our initial expectations, however, ab initio calculations indicate that this specificity arises from the dynamics of the molecule–surface reaction rather than the thermodynamic energies of the different surface adducts.

## II. Experimental Section

Experimental measurements were performed using scanning tunneling microscopy (STM) and Fourier transform infrared spectroscopy (FTIR). STM and FTIR experiments were performed in separate ultrahigh vacuum (UHV) chambers having base pressures  $<10^{-10}$  Torr.

Silicon wafers were purchased from Wacker. Two surface orientations were used. All STM and most FTIR experiments used “on-axis” samples that were oriented to  $(001) \pm 0.5^\circ$ . On-axis samples are characterized by large, flat terraces separated by steps that are one atomic layer in height, and have equal amounts of the equivalent  $(1 \times 2)$  and  $(2 \times 1)$  domains of dimer orientations. On-axis STM samples were highly doped ( $<0.1$  ohm cm, Sb doped), while on-axis FTIR samples were lightly doped ( $>5$  ohm cm, B-doped). A small number of FTIR experiments were performed using lightly doped ( $>5$  ohm cm, P-doped) “off-axis” wafers that were intentionally miscut by  $4.0 \pm 0.5^\circ$  off  $(001)$  in the  $\langle 110 \rangle$  direction; these samples are characterized by small ( $\sim 25$  Å) terraces separated by steps that are two atomic layers in height. All dimers on the off-axis wafers are oriented in a single direction. When used with polarized infrared light, off-axis samples yield information about the orientation of the molecules with respect to the Si=Si dimer bond. Unless otherwise stated, infrared spectra reported here were obtained on two-domain (on-axis) samples, using unpolarized light.

Wafers polished on both sides were used in all infrared spectroscopy experiments. From these large wafers individual smaller samples ( $\sim 1$  cm  $\times$  2 cm) were cut. The narrow edges ( $\sim 0.5$  mm  $\times$  1 cm) were then polished at a  $45^\circ$  angle. For all experiments, samples were degassed overnight at 840 K and then flash annealed to 1400 K until pressure stabilized at  $<3 \times 10^{-10}$  Torr, producing a clean  $(2 \times 1)$ -reconstructed surface.<sup>30</sup>

Infrared absorption spectra for attached molecules were obtained using a Mattson RS-1 FTIR spectrometer coupled to a UHV system through two BaF<sub>2</sub> windows. The infrared light was focused into the narrow edge of the trapezoidal samples. After propagating down the  $\sim 2$  cm length of the sample the light emerged from the narrow edge at the opposite end of the sample, where it was collected and focused on a liquid nitrogen-cooled InSb detector. Spectra were acquired with  $2$  cm<sup>-1</sup> resolution. In some experiments a wire-grid polarizer was used to define the direction of the electric field with respect to the sample. Liquid spectra were obtained using a Nicolet 740 FTIR with a triglycine sulfate (TGS) detector at  $1$  cm<sup>-1</sup> resolution.

Direct observation of adsorbed molecules was achieved with a home-built UHV scanning tunneling microscope (STM). While a range of imaging conditions was explored, all images shown here were obtained using a sample bias of  $-2.2$  V and a tunneling current of 80 pA.

Styrene was purchased from Aldrich (99+% purity). Two types of isotopically labeled styrene were purchased from Cambridge Isotopes Laboratories (both 98+% purity). In C<sub>6</sub>H<sub>5</sub>CD=CD<sub>2</sub> (referred to here as *d*<sub>3</sub>-styrene), the hydrogen atoms on the vinyl portion of the molecule were replaced with deuterium. In C<sub>6</sub>D<sub>5</sub>CH=CH<sub>2</sub> (referred to here as *d*<sub>5</sub>-styrene) the hydrogen atoms on the benzene ring were replaced with deuterium. All samples were further purified through freeze–pump–thaw cycles. Purity of the molecules was verified using mass spectrometers on each UHV chamber. The benzene and toluene spectra were described previously.<sup>45</sup>

In both vacuum chambers used for these studies, the styrene is introduced using a leak valve, and pressure is measured using an ionization gauge. The location of the leak valve and other geometric properties of the vacuum systems make the effective pressure at the sample higher than the background pressure rise detected by the ionization gauge. All pressures and doses reported here are based on the uncorrected background pressure measurement, and therefore the true exposures at the sample are expected to be several times higher.

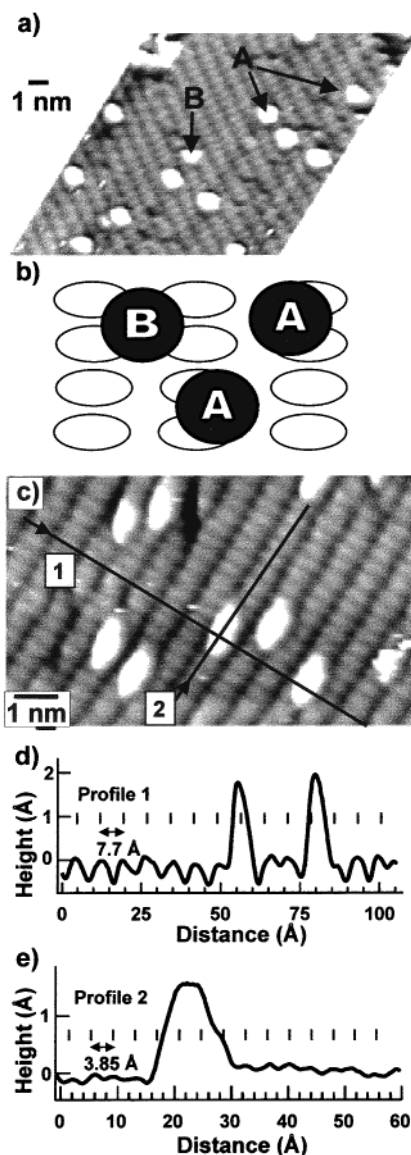


**Figure 2.** STM images, height contours, and schematic illustration of bonding configurations of observed features for styrene on Si(001). (a) STM image of the Si(001) surface exposed to 0.01 L of styrene; the image was acquired at a sample bias of  $-2.2$  V and a tunneling current of 80 pA; “A” and “B” refer to the two types of features observed. (b) Schematic illustration showing the approximate location of “A” and “B” features with respect to underlying dimers. (c) STM image showing type “A” features at higher resolution, after 0.01 L of exposure; the image was acquired at a sample bias of  $-2.2$  V and a tunneling current of 80 pA. (d) Height profile measured perpendicular to the dimer rows and extending over two type “A” features. (e) Height profile measured parallel to the dimer rows and extending over a single type “A” feature.

## III. Results

**A. STM Data.** Figure 2a shows a room-temperature STM image obtained after a clean Si(001) surface was exposed to 0.01 L ( $10^{-8}$  Torr for 1 s) of styrene. At low coverage, individual molecules can be imaged in their preferred adsorption geometry without steric interaction from other molecules. Two types of protrusions, labeled “A” and “B”, are visible, as depicted in Figure 2b. Feature “A” appears to be on a dimer row, but is shifted slightly to one side of the row. While such small deviations can sometimes be caused by asymmetric STM tips, the slight sideways shift occurs randomly on each side of the dimer rows, suggesting that it is related to inherent asymmetry

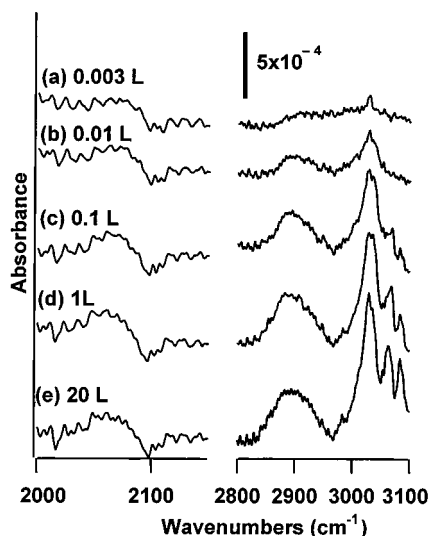


**Figure 3.** FTIR data for coverage dependence of styrene on the Si(001) surface at 114 K. Doses were (a) 0.003, (b) 0.01, (c) 0.1, (d) 1, and (e) 20 L.

in the structure of the surface-bound molecules. The feature spans approximately two dimers. Feature “B” is centered between dimer rows, and is approximately the same size as feature “A”. Counting statistics of several images indicate that there is one preferred bonding geometry (“A”), with some possibility of a second molecular feature or dissociation product (“B”) comprising less than 10% of the surface species. The asymmetry in local bonding of type “A” features can be observed more clearly in the STM image of Figure 2c and the corresponding STM height profiles shown in Figures 2d and 2e. Height profile 1 (Figure 2d) passes over two type “A” features, one of which is shifted to the left and the other of which is shifted to the right of the center of a dimer row. The apparent height of each feature is approximately 2 Å. The height profile in Figure 2d shows that the feature can extend along almost 4 dimers, but most of the apparent height is limited to the width of two dimers ( $\sim 8$  Å width).

**B. Vibrational Spectroscopy.** Figure 3 shows how the vibrational spectrum of styrene on silicon(001) varies with exposure. These spectra were obtained using an on-axis Si(001) sample that was cooled to 114 K, at exposures of (a) 0.003 L ( $3 \times 10^{-9}$  Torr for 1 s), (b) 0.01 L ( $1 \times 10^{-8}$  Torr for 1 s), (c) 0.1 L ( $1 \times 10^{-8}$  Torr for 10 s), (d) 1 L ( $1 \times 10^{-7}$  Torr for 10 s), and (e) 20 L ( $1 \times 10^{-7}$  Torr for 200 s) of styrene. A comparison of the spectra shows that all peaks increase uniformly in intensity until saturation is observed at an exposure of  $\sim 1$  L (Figure 3d). No significant changes in relative intensities are observed thereafter up through the highest exposure studied (20 L). There are three main regions of interest for these spectra. The 2965–3110  $\text{cm}^{-1}$  region shows three distinct peaks at 3028, 3062, and 3082  $\text{cm}^{-1}$ ; this is the region usually associated with C–H stretches of unsaturated and/or aromatic hydrocarbons. The second region shows a broad, structured peak centered at approximately 2896  $\text{cm}^{-1}$ ; this is within the spectral region usually associated with C–H stretches of saturated hydrocarbons. Finally, we note that there is no significant absorption in the region from 2000 to 2100  $\text{cm}^{-1}$ ; this is the region usually associated with Si–H stretches. The absence of measurable absorbance in this region suggests that there is little or no cleavage of C–H bonds during adsorption.

Figure 4 shows a comparison of the vibrational spectra for styrene (a, b),  $d_3$ -styrene (c, d), and  $d_5$ -styrene (e, f). For each

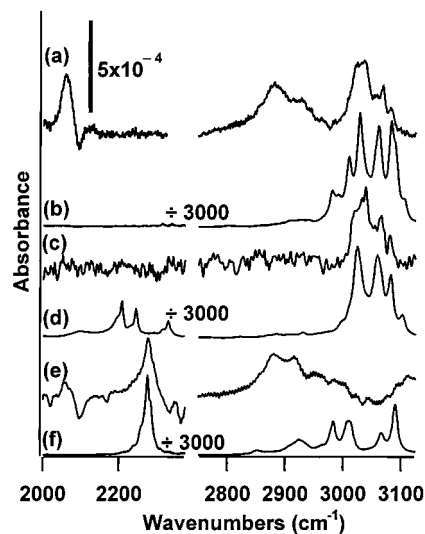


**Figure 4.** Comparison of liquid spectra with surface-bound spectra: (a) 10 L of styrene on Si(001) surface, (b) neat liquid styrene, (c) 10 L of  $d_3$ -styrene on Si(001) surface, (d) neat liquid  $d_3$ -styrene, (e) 10 L of  $d_5$ -styrene on Si(001) surface, and (f) neat liquid  $d_5$ -styrene.

**Table 1.** Comparison of Vibrational Data ( $\text{cm}^{-1}$ ) for Liquid and Surface Bound Styrene and Isotopically Substituted Styrene<sup>a</sup>

styrene		$d_3$ -styrene		$d_5$ -styrene	
surface-attached	neat liquid	surface-attached	neat liquid	surface-attached	neat liquid
2060				2060	
			2092		
			2208	2258 sh	2258 sh
			2245	2276	2276
			2328	2290 sh	2282 sh
2880				2874	2850
2926	2926			2916	2924
	2980				2984
	3010				3010
3036	3028	3038	3024		
3068	3060	3066	3060		3066
3080	3082	3082	3082		3090
			3102		

<sup>a</sup> sh indicates a shoulder on a larger peak.

isotope, spectra are shown for the molecule bound to the Si(001) surface (a, c, e), after 10 L exposure ( $5 \times 10^{-8}$  Torr for 200 s) at 300 K, and for the pure liquid (b, d, f). Table 1 summarizes the vibrational frequencies. In the neat liquids, many of the observed C–H vibrations are combination bands and involve extensive coupling between C–H vibrations of the ring and those of the vinyl group. Consequently, the modes are not readily attributed to one specific part of the molecule.<sup>46</sup>

Figure 4a shows vibrational spectroscopy data for 10 L of styrene adsorbed onto a Si(001) sample at 300 K. The 2700–3000  $\text{cm}^{-1}$  alkane C–H region shows a broad structure with at least two peaks at 2880 and 2926  $\text{cm}^{-1}$ . The alkene stretching region (3000–3100  $\text{cm}^{-1}$ ) shows three peaks at 3036, 3068, and 3080  $\text{cm}^{-1}$ . Finally, there is a peak at 2060  $\text{cm}^{-1}$  that arises from Si–H vibrations, indicating some partial dissociation on the surface. For comparison, Figure 4b shows the FTIR spectrum for liquid styrene. The pure liquid has alkene-like and aromatic stretching vibrations in the 3000–3100  $\text{cm}^{-1}$  region, but exhibits no significant absorption in the 2800–3000  $\text{cm}^{-1}$  region. Consequently, we conclude that vibrational modes in the 2800–3000  $\text{cm}^{-1}$  region arise as a consequence of bonding to the surface.

(46) Condirston, D. A.; Laposa, J. D. *J. Mol. Spectrosc.* **1976**, *63*.

The presence of the  $2060\text{ cm}^{-1}$  Si–H vibrational feature after Si(001) is exposed to styrene at 300 K indicates that there is some C–H bond cleavage during the adsorption process, leaving H atoms bonded to surface Si atoms. The absence of any detectable Si–H peak after adsorption onto the cold (114 K) sample then indicates that at low temperatures there is no significant C–H bond cleavage. The overall spectrum obtained on the 300 K sample (Figure 4a) appears quite similar to that of styrene adsorbed onto a 114 K sample (Figure 3). This suggests that either the extent of dissociation at 300 K is small or else that it has only minor impact on the C–H vibrational modes.

To estimate the extent of dissociation, the integrated absorbance of the Si–H region in this spectrum was compared to the integrated absorbance obtained on a Si(001)–( $2 \times 1$ )H monohydride surface that consists of one hydrogen atom per Si atom.<sup>47</sup> The integrated absorbance for the Si(001)–( $2 \times 1$ )H monohydride surface was  $0.11\text{ cm}^{-1}$ , while the integrated absorbance for the Si–H peak found in Figure 4a was  $\sim 0.01\text{ cm}^{-1}$ . Although hydrogen atoms produced by dissociation of styrene are more likely to be present in the form of a “hemihydride” (i.e., a silicon dimer in which there is only one hydrogen atom), *ab initio* calculations of the expected infrared intensities for the monohydride and hemihydride structures were found to be the same within approximately 20%. This then suggests that the Si–H peak in Figure 4a corresponds to  $\sim 9\%$  of a monolayer of adsorbed hydrogen.

Figure 4 show analogous FTIR spectra for  $d_3$ -styrene (c and d), in which the vinylic part of the molecule is deuterated. Figure 4c shows an unpolarized FTIR spectrum after the Si(001) surface was exposed to 10 L of  $d_3$ -styrene at room temperature. One important feature of this spectrum is the *absence* of any significant absorption in the  $2850\text{--}3000\text{ cm}^{-1}$  alkane region, while three strong absorption peaks are observed at higher frequencies of  $3038$ ,  $3066$ , and  $3082\text{ cm}^{-1}$ . These frequencies are identical (within the  $2\text{ cm}^{-1}$  resolution) to those found in the same region for unlabeled styrene bonded to Si(001) (Figure 4a), suggesting little or no direct interaction between the aromatic ring and the Si(001) surface. Also notable is that there is no detectable absorption at  $2060\text{ cm}^{-1}$  where Si–H vibrations are found nor in the  $2125\text{--}2275\text{ cm}^{-1}$  region where C–D vibrations from the vinyl group might be expected. The region where Si–D vibration might be observed is not spectrally accessible due to bulk silicon absorption. Figure 4d shows the FTIR spectrum for neat liquid  $d_3$ -styrene. Absorption peaks at  $3024$ ,  $3060$ ,  $3082$ , and  $3102\text{ cm}^{-1}$  arise from C–H vibrations on the aromatic ring, while peaks at  $2208$ ,  $2245$ , and  $2328\text{ cm}^{-1}$  arise from the C–D stretches of the vinyl group.<sup>46</sup>

Figure 4 shows the corresponding spectra for  $d_3$ -styrene (e and f), in which hydrogen atoms on the aromatic ring are replaced with deuterium. Figure 4e shows an unpolarized FTIR spectrum of an on-axis Si(001) surface exposed to 10 L of  $d_3$ -styrene at room temperature. This spectrum shows a broad set of alkane-like C–H vibrations extending from  $2834$  to  $2972\text{ cm}^{-1}$  with peaks at  $2874$  and  $2916\text{ cm}^{-1}$ . The overall shape of this group of vibrations appears similar to that obtained when unlabeled ( $\text{C}_6\text{H}_5\text{CH}=\text{CH}_2$ ) styrene (Figure 4a) is bonded to the surface, although there are some minor changes in intensity. Figure 4e also shows a set of C–D vibrations consisting of a peak at  $2276\text{ cm}^{-1}$  with shoulders at  $\sim 2258$  and  $2290\text{ cm}^{-1}$ , arising from the C–D stretches of the deuterated ring. Additionally, a small peak at  $2060\text{ cm}^{-1}$  is observed, arising from Si–H vibrations. A comparison of the spectrum obtained when

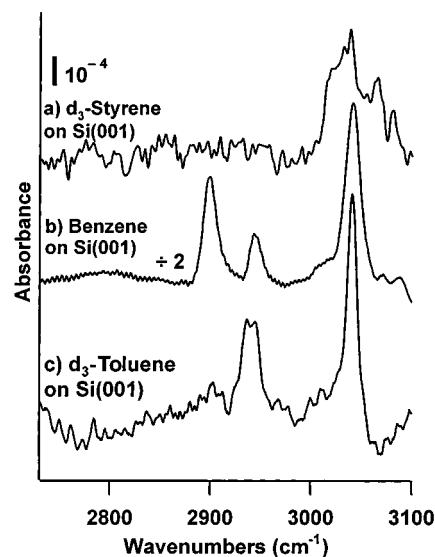


**Figure 5.** Comparison between (a) saturation coverage (10 L) of  $d_3$ -styrene, (b) saturation coverage (0.5 L) of benzene, and (c) saturation coverage (1.6 L) of  $d_3$ -toluene.

$\text{C}_6\text{D}_5\text{CH}=\text{CH}_2$  is bonded to the surface (Figure 4e) with the spectrum obtained when  $\text{C}_6\text{H}_5\text{CH}=\text{CH}_2$  is bonded to the surface (Figure 3a) shows that the absorption features between  $2976$  and  $3110\text{ cm}^{-1}$  are present only for  $\text{C}_6\text{H}_5\text{CH}=\text{CH}_2$ . Consequently, we attribute these features to C–H stretches of the aromatic ring of the surface-attached molecules.

Figure 4f shows a vibrational spectrum of neat liquid  $d_3$ -styrene. The C–D stretching vibrations at  $2276\text{ cm}^{-1}$  and weaker shoulders at  $2258$  and  $2282\text{ cm}^{-1}$  are virtually identical to those observed for  $d_3$ -styrene after attachment to the surface (Figure 4e). However, the C–H vibrations at  $2870\text{--}3100\text{ cm}^{-1}$  are very different for the neat liquid (Figure 4f) and the surface-bound  $d_3$ -styrene (Figure 4e) spectra. In particular, we note that the high-frequency peak observed at  $3090\text{ cm}^{-1}$  for neat  $d_3$ -styrene (Figure 4f) is completely eliminated upon adsorption to the surface (Figure 4e).

Since styrene can, in principle, bond either through the aromatic ring or through the external vinyl group, we also obtained infrared spectra of two related systems: benzene and  $\text{C}_6\text{H}_5\text{--CD}_3$  ( $d_3$ -toluene). Figure 5 shows spectra of Si(001) exposed to (a) 10 L of  $d_3$ -styrene, (b) 0.5 L of benzene, and (c) 1.6 L of  $d_3$ -toluene. Previous studies have shown that bonding of benzene and toluene occurs through the aromatic ring system,<sup>41–45,48</sup> thereby destroying its aromaticity. This can be seen quite clearly by the fact that the spectra of benzene (Figure 5b) and toluene (Figure 5c) have strong vibrational modes at  $<3000\text{ cm}^{-1}$ . Specifically, there are distinct peaks at  $2899$  and  $2944\text{ cm}^{-1}$  for benzene and a peak at  $2940\text{ cm}^{-1}$  for toluene.<sup>41,43,45</sup> In contrast, the spectrum of  $d_3$ -styrene is dominated by high-frequency modes very similar to those of the unperturbed aromatic ring.

To identify whether styrene molecules exhibit any preferred orientation in the surface plane, s- and p-polarized spectra were obtained on “off-axis” Si(001) surfaces purposely miscut by  $4^\circ$  toward the [110] direction. As noted earlier, this surface consists of short terraces with all dimers in a single ( $2 \times 1$ ) domain. Figure 6 shows the four spectra obtained. While the s-polarized spectra can be aligned with the electric field vector parallel to one of the principal lattice directions, p-polarized spectra contain a mixture of in-plane and out-of-plane components, as indicated.

(47) Sakurai, T.; Hangstrom, H. D. *Phys. Rev. B* **1976**, *14*, 1593.

(48) Craig, B. I. *Surf. Sci.* **1993**, *280*, L279–L284.

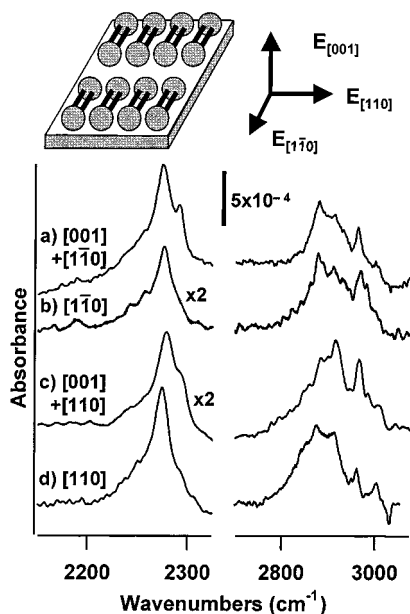


**Figure 6.** Polarization-dependent spectra for  $d_5$ -styrene on Si(001) and schematic depiction of orientation directions: (a)  $d_5$ -styrene with light polarized in the  $\langle 1\bar{1}0 \rangle$  and  $\langle 001 \rangle$  directions, (b)  $d_5$ -styrene with light polarized in the  $\langle 110 \rangle$  direction, (c)  $d_5$ -styrene with light polarized in the  $\langle 110 \rangle$  and  $\langle 001 \rangle$  directions, and (d)  $d_5$ -styrene with light polarized in the  $\langle 110 \rangle$  direction.

The only significant, reproducible difference between the spectra in Figure 6 is that when the electric field vector of the infrared light is along the  $\langle 001 \rangle$  direction (i.e., along the surface normal) (Figure 6, a and c) there is a small shoulder at  $2292\text{ cm}^{-1}$  that is not evident in the other spectra (Figure 6, b and d). This polarization-dependent change indicates that there is some preferential alignment of the aromatic ring with respect to the surface normal. However, the overall influence of the polarization of the light is much less pronounced than in previous studies of benzene, toluene, and xylenes adsorbed on Si(001).<sup>45</sup>

Since previous studies have shown that at elevated temperatures benzene will desorb from Si(001)<sup>41,42</sup> while nonaromatic systems undergo fragmentation,<sup>6,49</sup> spectra were obtained after the  $d_3$ -styrene exposed Si(001) sample was heated to elevated temperatures. Figure 7 shows FTIR spectra for (a) a 10 L dose of  $d_3$ -styrene at 300 K, followed by heating of the silicon surface to (b) 350, (c) 500, and (d) 700 K. The samples were allowed to cool to 300 K before spectra were taken. Two changes are evident after heating to 500 and 700 K: (1) the addition of a peak at  $2060\text{ cm}^{-1}$  and (2) a distinct change in vibrational peaks in the  $2994\text{--}3096\text{ cm}^{-1}$  region. In particular, a peak appears at  $3056\text{ cm}^{-1}$ , and the peaks originally at  $3038$ ,  $3066$ , and  $3080\text{ cm}^{-1}$  are either reduced or disappear altogether.

**C. Ab Initio Calculations.** To understand the different bonding energies, we performed ab initio calculations for styrene interacting with clusters of silicon atoms representing the (001) surface. Figure 8 shows  $\text{Si}_9\text{H}_{12}$  and  $\text{Si}_{15}\text{H}_{16}$  clusters that were used to simulate the Si(001) surface. The  $\text{Si}_9\text{H}_{12}$  cluster has two exposed atoms that are bonded together in a geometry very similar to that of a single dimer on the Si(001) surface. Similarly, the  $\text{Si}_{15}\text{H}_{16}$  cluster has four exposed atoms that are in a geometry very similar to that of two adjacent dimers of the Si(001) surface. Hydrogen atoms were added as needed to ensure 4-fold coordination of all Si atoms except the exposed dimers. While most calculations of bonding geometry were performed using

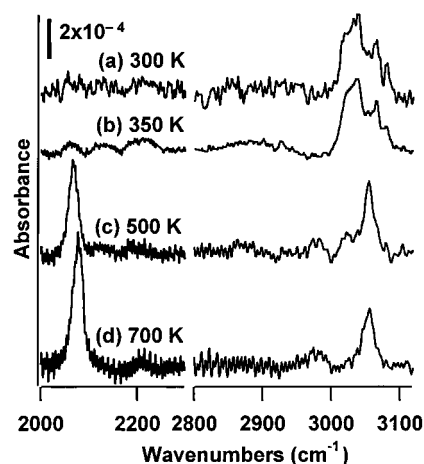


**Figure 7.** FTIR spectra for (a) exposure to 10 L of  $d_3$ -styrene at 300 K followed by heating to (b) 350, (c) 500, and (d) 700 K. The original sample dosed at 300 K was heated for 120 s to the indicated temperatures and then allowed to cool back to 300 K before spectra were acquired.

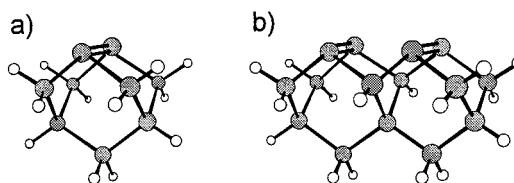


**Figure 8.**  $\text{Si}_9\text{H}_{12}$  and  $\text{Si}_{15}\text{H}_{16}$  clusters used to model the Si(001) surface. All dangling bonds except those on the dimerized surface atoms are removed by terminating with hydrogen atoms, as shown.

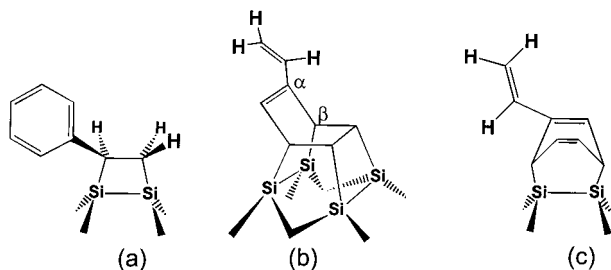
the large  $\text{Si}_{15}\text{H}_{21}$  cluster, some calculations were performed with the smaller cluster to achieve faster computation time and to permit exploring a larger number of geometries. All calculations utilized the Gaussian 98 program.<sup>50</sup>

Figure 9 shows three potential bonding geometries for styrene attached to the Si surface. Using the 6-31+G\* basis set, the Becke3LYP density functional, and the  $\text{Si}_{15}\text{H}_{16}$  cluster,<sup>51</sup> we calculated the binding energy of styrene through the vinyl group (Figure 9a) to be  $154\text{ kJ/mol}$  ( $1.60\text{ eV}$ ,  $37\text{ kcal/mol}$ ). The interaction of the aromatic ring with two adjacent dimers in a configuration known as the “tight bridge” geometry (Figure 9b)<sup>41</sup> yields a binding energy of  $156\text{ kJ/mol}$  ( $1.62\text{ eV}$ ,  $37\text{ kcal/mol}$ ). Bonding with a single dimer via a [4+2] interaction of the

(49) Kong, M. J.; Teplyakov, A. V.; Jagmohan, J.; Lyubovitsky, J. G.; Mui, C.; Bent, S. F. *J. Phys. Chem. B* **2000**, *104*, 3000–3007.

(50) Frisch, M. J.; Trucks, G. W.; Schlegel, H. B.; Scuseria, G. E.; Robb, M. A.; Cheeseman, J. R.; Zakrzewski, V. G.; Montgomery, J. A.; Stratmann, R. E.; Burant, J. C.; Dapprich, S.; Millam, J. M.; Daniels, A. D.; Kudin, K. N.; Strain, M. C.; Farkas, O.; Tomasi, J.; Barone, V.; Cossi, M.; Cammi, R.; Mennucci, B.; Pomelli, C.; Adamo, C.; Clifford, S.; Ochterski, J.; Petersson, G. A.; P. Y. Ayala, Q. C.; Morokuma, K.; Malick, D. K.; Rabuck, A. D.; Raghavachari, K.; Foresman, J. B.; Cioslowski, J.; Ortiz, J. V.; Stefanov, B. B.; Liu, G.; Liashenko, A.; Piskorz, P.; Komaromi, I.; Gomperts, R.; Martin, R. L.; Fox, D. J.; Keith, T.; Al-Laham, M. A.; Peng, C. Y.; Nanayakkara, A.; Gonzalez, C.; Challacombe, M.; Gill, P. M. W.; Johnson, B. G.; Chen, W.; Wong, M. W.; Andres, J. L.; Head-Gordon, M.; Replogle, E. S.; Pople, J. A. *GAUSSIAN 98*; Revision A.1 ed.; Frisch, M. J.; Trucks, G. W.; Schlegel, H. B.; Scuseria, G. E.; Robb, M. A.; Cheeseman, J. R.; Zakrzewski, V. G.; Montgomery, J. A.; Stratmann, R. E.; Burant, J. C.; Dapprich, S.; Millam, J. M.; Daniels, A. D.; Kudin, K. N.; Strain, M. C.; Farkas, O.; Tomasi, J.; Barone, V.; Cossi, M.; Cammi, R.; Mennucci, B.; Pomelli, C.; Adamo, C.; Clifford, S.; Ochterski, J.; Petersson, G. A.; P. Y. Ayala, Q. C.; Morokuma, K.; Malick, D. K.; Rabuck, A. D.; Raghavachari, K.; Foresman, J. B.; Cioslowski, J.; Ortiz, J. V.; Stefanov, B. B.; Liu, G.; Liashenko, A.; Piskorz, P.; Komaromi, I.; Gomperts, R.; Martin, R. L.; Fox, D. J.; Keith, T.; Al-Laham, M. A.; Peng, C. Y.; Nanayakkara, A.; Gonzalez, C.; Challacombe, M.; Gill, P. M. W.; Johnson, B. G.; Chen, W.; Wong, M. W.; Andres, J. L.; Head-Gordon, M.; Replogle, E. S.; Pople, J. A., Ed.; Gaussian Inc.: Pittsburgh, 1998.

(51) Lee, C.; Wang, W.; Parr, R. G. *Phys. Rev. B* **1988**, *37*, 785.



**Figure 9.** Geometries for ab initio calculations: (a) styrene in [2+2] geometry bonding through the vinyl group; (b) styrene in “tight bridge” geometry bonding through the aromatic ring; and (c) styrene in [4+2] geometry bonding through the aromatic ring.

aromatic ring (Figure 9c) yields a binding energy of 81 kJ/mol (0.84 eV, 19 kcal/mol). These energies are similar to those reported previously for benzene using the same Becke3LYP density functional method with the slightly smaller 6-31G\* basis set.<sup>52</sup> The earlier calculations for benzene yielded binding energies of 143 kJ/mol (1.49 eV, 34 kcal/mol) in the “tight bridge” configuration and 85 kJ/mol (0.88 eV, 20 kcal/mol) in the [4+2] configuration,<sup>52</sup> compared with our values for styrene of 156 (1.62 eV, 37 kcal/mol) and 81 kJ/mol (0.84 eV, 19 kcal/mol) in similar configurations. The earlier calculations for benzene also considered additional configurations such as a [2+2] reaction with the aromatic ring and a low-symmetry two-dimer configuration known as a “twist-bridge”.<sup>52</sup> Because the benzene calculations showed these to be very high-energy configurations, we did not consider the analogous configurations for styrene.

For styrene, the tight-bridge configuration has three different possible variations and the [4+2] configuration has two variations, differing in the location of the vinyl group around the ring. Two optimization calculations were performed to compare the total energy of the tight bridge configuration with the vinyl group in the  $\alpha$  to the  $\beta$  position indicated in Figure 9b. Moving the vinyl group from the  $\alpha$  to the  $\beta$  position caused the bonding energy to be reduced from 156 kJ/mol (1.62 eV, 37 kcal/mol) to 121 kJ/mol (1.25 eV, 29 kcal/mol); we attribute this energy difference primarily to the fact that when the vinyl group is in the  $\alpha$  position it is conjugated to another C=C bond, and when in the  $\beta$  position it is not. Because we expect that the binding energy should always be highest when the vinyl group retains conjugation to at least one double bond, we limited our calculations to the configurations that retain as much conjugation as possible, as depicted in Figure 9. Perhaps the most important result from our ab initio calculations is that they show that there is *not* a strong thermodynamic preference for bonding via the aromatic ring into a tight bridge configuration (Figure 9b) compared to binding through the vinyl group into a [2+2] adduct (Figure 9a). A similar conclusion has also been reached for studies of phenyl isothiocyanate ( $C_6H_5-N=C=S$ ) on Si(001), which also undergoes a cycloaddition reaction with Si(001) through the N=C bond.<sup>53</sup>

Since previous studies have found that interaction of alkenes with Si(001) and Ge(001) likely occurs through a low-symmetry configuration in which the molecule interacts with the end of a dimer,<sup>24,39</sup> we also performed calculations in which either the aromatic ring or the vinyl group was placed near the end of a dimer, as depicted in Figure 10. These calculations were performed at the Hartree–Fock level using the 6-31 basis set.

(52) Wolkow, R. A.; Lopinski, G. P.; Moffatt, D. J. *Surf. Sci.* **1998**, *416*, L1107–L1113.

(53) Ellison, M. D.; Hamers, R. J. *J. Phys. Chem. B* **1999**, *103*, 6243–6251.

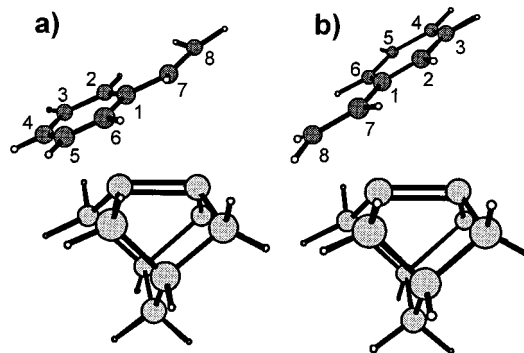


**Figure 10.** (a) Interaction of styrene with Si(001) in low-symmetry geometry via the vinyl group. (b) Interaction of styrene with Si(001) in low-symmetry geometry via the aromatic ring.

For each initial geometry a constrained energy minimization was then performed in which the distance between the Si atom at the end of the dimer and the nearest C atom of styrene (atom 1, 4, 7, or 8, depending on the calculation) was held at a fixed distance, while all other degrees of freedom were unconstrained. These calculations showed that when the C atom nearest the dimer was part of the aromatic ring (atoms 1 or 4 nearest the dimer end, as depicted in Figure 10a), the total energy increased. In contrast, if the C atom was part of the vinyl group (atoms 7 or 8 nearest the dimer end, as depicted in Figure 10b), then the energy was lowered by 0.2–0.3 eV (20–30 kJ/mol). A number of calculations were performed, keeping atom 1, 4, 7, or 8 at a distance of 2.5 or 3.0 Å from the dimer end. In each case tried, the calculations showed that the interaction with the vinyl group produced a substantial lowering of the energy, while interaction with the aromatic ring led to a slight increase in the energy. These results suggest that the interaction of styrene with the surface is energetically favorable if the vinyl group interacts with a surface dimer, but is energetically neutral or repulsive if the aromatic ring interacts with the surface dimer. Therefore, while our calculations suggest that there is no strong thermodynamic preference for bonding through the vinyl group or the aromatic ring, it appears that bonding through the vinyl group may be favored by a long-range attractive interaction between the vinyl group and the surface dimers.

#### IV. Discussion

**Adsorption Geometry.** The experimental data above reveal several pieces of information important in establishing the bonding geometry. First, we note that STM images (Figure 2) at 300 K show that more than 90% of the molecules appear to be in a single bonding geometry. From the STM data alone, however, definitive assignment of a bonding configuration is not possible. The off-center position of the observed feature is consistent with all three principal bonding configurations. While a detailed calculation of the STM images for each configuration might help in elucidating the molecular structure, uncertainty in the electronic and geometric structure of the tip can make detailed identification tenuous. Since the STM data show that the vast majority of molecules bond into a single configuration, however, infrared data can be obtained and then analyzed in terms of a single dominant surface adduct.

The FTIR data in Figure 3 show that adsorption onto a cold (114 K) surface produces no significant Si–H vibrational intensity at 2000–2100  $cm^{-1}$ . This demonstrates that at low temperatures, adsorption occurs without cleavage of C–H bonds. Cleavage of C–H bonds can be detected in FTIR through the appearance of Si–H vibrations, because the H atoms

detached from adsorbed molecules cannot readily leave the surface as H<sub>2</sub> and instead bond to the underlying Si surface. Although bonding to a Si(001) surface at room temperature does produce some C–H bond fragmentation, the extent of fragmentation (no more than 0.09 monolayer) appears sufficiently small that it does not impact the C–H region significantly. The uniform increases in all C–H vibrational peak intensities (2800–3110 cm<sup>-1</sup>) as the exposure is increased up to saturation indicate that the vibrational spectra are not dependent on coverage, and that intermolecular coupling does not significantly affect the vibrational spectra.

Comparing the spectra of the isotopically labeled components shows that the predominant interaction with the surface occurs through the vinyl group, rather than through the aromatic ring. The fact that the low-frequency vibrational modes at 2850–2980 cm<sup>-1</sup> for unlabeled styrene adsorbed on Si(001) (Figure 4a) are absent for adsorbed *d*<sub>3</sub>-styrene (Figure 4c) and present for adsorbed *d*<sub>5</sub>-styrene (Figure 4e) proves that these modes arise from the vinylic portion of the molecule. The absence of these modes for the neat styrene spectrum, in turn, indicates that they are a direct result of the interaction of the vinyl group with the surface. We note that the spectrum of C<sub>6</sub>H<sub>5</sub>–CD=CD<sub>2</sub> does not show any C–D vibrations at 2110–2150 cm<sup>-1</sup> where the alkane-like C–D vibrations would be expected based on the different reduced mass of C–D compared with CH. However, the alkane-like C–H vibrations for chemisorbed unlabeled styrene (Figure 4a) are quite broad, and we attribute their absence in Figure 4c to their breadth and because the isotope effect is expected to make the integrated intensity of the C–D infrared only half the intensity of the comparable C–H stretch.<sup>54</sup> Thus, we conclude that the interaction of styrene with the Si(001) surface involves the vinyl group.

To determine whether the vinyl group alone interacts with the surface or whether the aromatic ring also interacts with the surface, we note that the high-frequency C–H stretching modes at >3000 cm<sup>-1</sup> are nearly identical for normal styrene (Figure 4a) and *d*<sub>3</sub>-styrene (Figure 4c), and are completely absent for *d*<sub>5</sub>-styrene (Figure 4e), when each molecule is bonded to the Si(001) surface. This comparison demonstrates that the >3000 cm<sup>-1</sup> modes arise almost entirely from the aromatic ring. We further note that the C–H stretching region of *d*<sub>3</sub>-styrene attached to the surface is nearly identical to that of *d*<sub>3</sub>-styrene liquid, and that the C–D stretching region of *d*<sub>5</sub>-styrene attached to the surface is nearly identical to that of *d*<sub>5</sub>-styrene liquid. These observations suggest that the aromatic ring is almost completely unperturbed by bonding of styrene to the Si(001) surface.

A comparison of the spectra of *d*<sub>3</sub>-styrene, benzene, and *d*<sub>3</sub>-toluene bonded to the Si(001) surface (Figure 5) further supports the *absence* of ring involvement in attachment of styrene to the Si(001) surface. Previous studies of benzene have shown that adsorption to Si(001) is complex.<sup>22,41–45,48</sup> Scanning tunneling microscopy images show at least two distinct types of adsorbed species, with transitions from one configuration to another occurring on time scales of minutes.<sup>22,41,42</sup> Similarly, vibrational spectroscopy measurements show changes in the distribution between adsorbed species as a function of temperature, but with no evidence for any C–H bond cleavage.<sup>45</sup> The infrared spectrum of free benzene in the liquid phase shows high-frequency peaks in the range of ~2987–3132 cm<sup>-1</sup>.<sup>55,56</sup> When adsorbed onto the Si(001) surface, however, benzene

shows the development of strong, sharp peaks at 2899 and 2944 cm<sup>-1</sup>, while also retaining some higher-frequency modes between 3000 and 3056 cm<sup>-1</sup>, as shown in Figure 5b. The presence of the alkane-like peaks at 2899 and 2944 cm<sup>-1</sup> for chemisorbed benzene is significant because such low-frequency C–H modes indicate that the aromatic nature of the ring is lost upon chemisorption.<sup>41,43,45</sup> Similarly, the infrared spectrum for *d*<sub>3</sub>-toluene shown in Figure 5c as well as spectra of isotopically labeled (C<sub>6</sub>H<sub>5</sub>–CD<sub>3</sub>) *o*-, *m*-, and *p*-xylenes<sup>45</sup> all show formation of alkane-like stretching vibrations at 2800–3000 cm<sup>-1</sup> due to loss of aromaticity of the benzene ring. While the experimental data are insufficient to definitively determine the bonding geometry of benzene on Si(001), the experimental data and ab initio total energy calculations suggest that one observed bonding geometry is a [4+2] adduct similar to that shown for styrene in Figure 9c.<sup>41,43,45,52</sup> The second geometry is believed to be a low-symmetry “tight bridge” configuration in which one benzene molecule interacts with two dimers within a single dimer row, similar to the structure shown for styrene in Figure 9b.<sup>41,43,45,52</sup>

These previous studies show that benzene, toluene, and xylene all bond to the Si(001) surface with formation of Si–C bonds, and that bonding to the surface is accompanied by loss of aromaticity.<sup>45</sup> For these molecules, however, the only readily accessible reactive site is the aromatic ring. In contrast, the infrared spectra of chemisorbed *d*<sub>3</sub>-styrene (Figure 5a) shows no evidence for alkane-like C–H vibrational modes. Instead, the surface-bound *d*<sub>3</sub>-styrene shows only high-frequency vibrational features at 3039, 3065, and 3081 cm<sup>-1</sup> that are nearly identical to those of liquid *d*<sub>3</sub>-styrene (Figure 4d). This observation strongly suggests that chemisorption of styrene to Si(001) leaves the aromatic ring intact and relatively unperturbed.

For chemisorbed *d*<sub>5</sub>-styrene we observe no significant absorption above 2932 cm<sup>-1</sup>, but observe two peaks at ~2874 and ~2916 cm<sup>-1</sup>. The latter two peaks can have two origins. First, they can arise from the C–H stretching modes of the vinyl group after bonding to the surface. For comparison, ethylene bonded to Si(001) gives rise to vibrational modes at 2883 and ~2920–2930 cm<sup>-1</sup>.<sup>17</sup> However, we note that liquid *d*<sub>5</sub>-styrene also shows C–H vibrations in the 2950–3100 cm<sup>-1</sup> region that arise from combination bands.<sup>46</sup>

The above observations lead us to conclude that styrene attaches almost exclusively through the vinyl group, with the aromatic ring left virtually unperturbed. To address the issue of whether the attaching vinyl group is intact or not, we note that FTIR spectra show that some Si–H stretching vibrations are detectable at 2060 cm<sup>-1</sup> when using normal styrene and when using *d*<sub>5</sub>-styrene, but not when using *d*<sub>3</sub>-styrene. However, a cold sample exposed to styrene showed no evidence for Si–H absorption. These observations lead us to conclude that (1) C–H bond cleavage is thermally activated and (2) C–H bond cleavage arises primarily from the vinyl group and not from the aromatic ring.

While a small amount of dissociation is detected at 300 K, quantitative analysis of the Si–H vibrational intensity shows that these surface-bound H atoms constitute less than 0.09 monolayer. Similarly, the STM images show only one primary chemisorbed species. Consequently, we conclude that while dissociation via cleavage of a C–H bond of the vinyl group is a minor, thermally activated pathway, the vast majority of the molecules bond to the surface through the vinyl group without C–H bond fragmentation.

**Symmetry Rules and Cycloaddition Reactions.** A particularly notable result of these experiments is that styrene shows

(54) Harmony, M. D. *Introduction to Molecular Energies and Spectra*; Holt, Rinehart, and Winston: New York, 1972.

(55) Galabov, B.; Ilieva, S.; Gounev, T.; Steele, D. *J. Mol. Struct.* **1992**, *273*, 85–98.

(56) Varsanyi, G. *Vibrational Spectra for Benzene Derivatives*; Academic Press: New York, 1969.



a high degree of selectivity in bonding to the surface, strongly preferring interaction through the vinyl group rather than the aromatic ring. This strong selectivity is surprising in light of the fact that bonding into the tight bridge configuration is predicted to have nearly the same enthalpy change (156 kJ/mol, 1.62 eV) as bonding through the vinyl group (154 kJ/mol, 1.60 eV). Binding through the aromatic ring has an energetic cost associated with the loss of aromaticity. As in the case of benzene, however, this energy cost is predicted to be more than offset by the energy gained in forming as many as four Si–C bonds in a “tight bridge” configuration (Figure 9b) or two Si–C bonds in a [4+2] configuration (Figure 9c). Bonding through the vinyl group via a [2+2] process (Figure 9a) retains the aromaticity of the ring, but creates only two Si–C bonds in a somewhat strained four-member  $\text{Si}_2\text{C}_2$  ring at the interface. The ab initio calculations indicate that these tradeoffs in energy are similar, so that there is no strong thermodynamic preference for bonding through either the vinyl group or the aromatic ring.<sup>57</sup>

While these calculations predict only small differences in energy between the different possible bonding configurations, they also reveal that the forces experienced by an impinging molecule depend strongly on the orientation of the molecule with respect to the surface. The initial (i.e., long-range) interaction of the vinyl group with the end of a Si=Si dimer is attractive, while the interaction of the aromatic ring was repulsive or essentially noninteracting for all the initial geometries utilized in the calculations. These results lead us to conclude that the selectivity for bonding through the vinyl group is *kinetic* in origin.<sup>58</sup>

To understand how the reaction dynamics controls cycloaddition reactions at Si(001) surfaces, it is important to understand the applicability of Woodward–Hoffmann rules to the “forbidden” [2+2] reactions, and how this might permit reaction of the vinyl group with the Si=Si dimers. According to Woodward–Hoffmann rules, the high-symmetry approach of two alkenes in a suprafacial–suprafacial geometry is forbidden, due to the fact that the symmetry of the ground electronic state correlates with an excited state of the final [2+2] product. The antarafacial–antarafacial approach is symmetry-allowed but in most cases is strongly sterically hindered, especially with bulky substituent groups. Consequently, thermal (i.e., nonphotochemical) [2+2] reactions between conventional alkenes are typically slow. However, the reactions of simple alkenes with the  $\pi$ -bonded Si(001)<sup>1–3,5,8–12,14,17,19,22,26,27,59,60</sup> and Ge(001)<sup>21,38</sup> surfaces to produce [2+2]-like products are facile. In fact, the probability of reaction per molecule–surface encounter (the reactive sticking coefficient) for cyclopentene is nearly unity on Si(001) and  $\sim 0.1$  on the Ge(001) surface, suggesting little or no barrier to adsorption.<sup>6</sup> Even the diamond(001) surface undergoes a [2+2] reaction with cyclopentene, albeit with a much lower reactive sticking coefficient on the order of  $10^{-3}$ .<sup>24,25</sup>

Since reactivity in [2+2] cycloaddition reactions is controlled by the alignment of the highest-occupied and lowest-unoccupied molecular orbitals of reactants, it is possible that the facile nature of [2+2] reactions of alkenes on Si(001) surfaces might be

(57) A similar selectivity was observed previously for phenyl isothiocyanate (PITC,  $\text{C}_6\text{H}_5\text{—N=C=S}$ ) on Si(001). Computational chemistry results for PITC on Si(001) showed no strong thermodynamic preference for bonding via a [2+2] reaction of the N=C bond or into benzene-like “tight bridge” configuration through the aromatic ring; experimental measurements showed that at low temperatures adsorption occurred almost exclusively through the N=C bond, leaving the aromatic ring unperturbed. See ref 53.

(58) A similar conclusion has been reached by Choi and Gordon in understanding selectivity between [2+2] and [4+2] reactions between conjugated dienes and the Si(001) surface. See ref 39.

attributed to intrinsic differences in the interacting molecular orbitals that might make the reactions allowed. However, recent theoretical studies have shown that [2+2] cycloadditions between alkenes and Si(001) via a high-symmetry suprafacial–suprafacial approach are expected to have a large barrier,<sup>39</sup> consistent with Woodward–Hoffmann symmetry rules. The observation of facile reactions despite a large barrier for a high-symmetry approach leads to the conclusion that the [2+2] reactions on Si(001) surfaces almost certainly occur through a *low-symmetry* pathway, for which Woodward–Hoffmann rules do not apply. This is further supported by the fact that ab initio calculations show that the interaction between the vinyl group of styrene with the end of a Si=Si dimer (similar to that shown in Figure 10b) is attractive at large separations. Similar conclusions have been reached for other alkenes<sup>24</sup> and for [2+2] reactions of conjugated dienes.<sup>39</sup>

Ultimately, we believe that the ability of Si(001) surfaces to undergo reactions of this type is connected with the fact that the bonds between the dimers and the underlying substrate are not planar (Figure 1a), and that tilting of the dimer unit creates an additional charge transfer making the “down” atom positively charged and the “up” atom negatively charged. The distortion from the planar configuration makes the unoccupied  $\pi^*$  orbital (located near the ends of the Si=Si dimers) very accessible to reactants and leads to a region of electron-deficiency at the “dangling bond” positions. When the Si=Si dimer tilts, the “down” atom becomes positively charged (as its geometry becomes more like the planar  $\text{SiH}_3^+$  ion<sup>61</sup>) and the “up” atom becomes negatively charged (as its geometry becomes more like that of the pyramidal  $\text{SiH}_3^-$  ion<sup>62</sup>). The “down” atom of a tilted dimer therefore has a pronounced decrease in electron density, making it an ideal site for attack by an electron-rich, nucleophilic reactant such as the vinyl group of styrene. We propose that the reactions of C=C unsaturated bonds with the Si(001) surface can be thought of as a nucleophilic addition reaction in which the electron-rich alkene interacts with the electron-deficient edge of a Si=Si dimer, and that this interaction is further facilitated by the ability of the dimers to tilt as the Si–C bond is formed.

The link between dimer reactivity and dimer tilting can be strengthened by noting that Si(001), Ge(001), and C(001) (diamond) surfaces all involve very similar dimer reconstructions, but exhibit large differences in reactivity in cycloaddition reactions with alkenes.<sup>24</sup> Dimers on Si(001) and Ge(001) surfaces can easily tilt out of the surface plane<sup>63</sup> and also show high reactivity toward alkenes such as cyclopentene, forming a [2+2]-like adduct.<sup>22,23</sup> In contrast, dimers on the C(001) (diamond) surface do *not* readily tilt out of the surface plane,<sup>64</sup> and the diamond(001) surface shows comparatively low reactivity toward cyclopentene.<sup>24</sup> This low reactivity occurs despite the fact that total energy calculations show that the bonding of cyclopentene to diamond is much more energetically favorable than bonding to Si(001) or Ge(001).<sup>24</sup> These results lead us to believe that the reactions are controlled by the dynamics of the molecule–surface interaction, and that dimer tilting likely plays an important role in facilitating the reaction.

We further note that the Si=Si bonds of the Si(001) surface are similar to the Si=Si bonds of disilenes, and that this

(59) Hovis, J.; Lee, S.; Liu, H.; Hamers, R. J. *J. Vac. Sci. Technol. B* **1997**, *15* (4), 1153–1158.

(60) Waltenberg, H. N.; Yates, J. T., Jr. *Chem. Rev.* **1995**, *95*, 1589–1673.

(61) Roszak, S.; Leszczynski, J. *Chem. Phys. Lett.* **1999**, *314*, 333–340.

(62) Shen, M.; Xie, Y.; H. F. S., III *J. Chem. Phys.* **1990**, *93*, 8098.

(63) Kubby, J. A.; Boland, J. J. *Surf. Sci. Rep.* **1996**, *26*, 61–204.

(64) Hukka, T. I.; Pakkanen, T. A.; D’Evelyn, M. P. *J. Phys. Chem.* **1994**, *98*, 12420–12430.

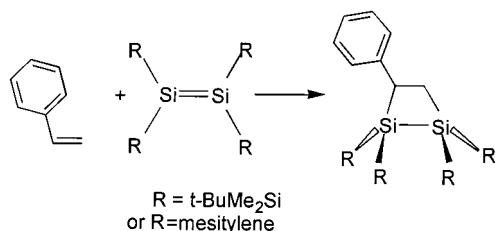


**Figure 11.** Reaction of styrene with tetramesityldisilene and tetra-*t*-butyldisilene.

structural similarity leads to similarity in their chemical behavior. While the Si=Si bonds at the Si(001) surface are distorted out of a planar configuration by the underlying bulk crystal lattice, similar distortions occur spontaneously for many disilenes. In H<sub>2</sub>Si=SiH<sub>2</sub>, for example, the Si–H bonds are bent 12.9° away from planarity in a *trans* configuration, as shown in Figure 1c.<sup>35</sup> Styrene reacts with tetramesityldisilene and also with tetrakis-(dimethyl-*tert*-butylsilyl)disilene to form [2+2] adducts through the vinyl group, as depicted in Figure 11.<sup>32,33,65</sup> In contrast, benzene reacts with tetramethyldisilene *only upon illumination*,<sup>66</sup> producing a [4+2] adduct similar to the initial configuration proposed for benzene adsorbed on Si(001). These results suggest that while the aromatic ring of benzene (and presumably styrene) can form stable (or metastable) adducts with Si=Si double bonds, bonding of the aromatic ring to the Si=Si bonds of disilenes appears to have a barrier that must be overcome. For both disilenes and the Si(001) surface, the net result is that bonding occurs preferentially through the vinyl group. Our proposed low-symmetry pathway is further supported by the

(65) Iwamoto, T.; Sakurai, H.; Kira, M. *Bull. Chem. Soc. Jpn.* **1998**, *71*, 2741–2747.

(66) Sekiguchi, A.; Maruki, I.; Ebata, K.; Kabuto, C.; Sakurai, H. *J. Chem. Soc. Commun.* **1991**, 341–343.

fact that the reaction of styrene with tetramesityldisilene occurs with partial loss of stereochemistry, implying a zwitterionic or radical intermediate.<sup>33</sup> While reactions of ethylene and butene on the Si(001) surface have been shown to *preserve* the stereochemistry,<sup>2,17</sup> it is likely that the aromatic ring in styrene may be particularly efficient in stabilizing a radical intermediate, thereby leading to greater loss of stereochemistry.

## V. Conclusions

This study shows that there is a strong selectivity in the adsorption of styrene to the Si(001) surface, almost entirely favoring bonding through the vinyl group. *Ab initio* calculations indicate that this selectivity originates in the fact that the interaction between the  $\pi$  electrons of the vinyl group and the end of a Si=Si dimer is attractive at comparatively large separations, thereby favoring bonding into a [2+2] adduct through a low-symmetry pathway. Reaction through this pathway does not violate Woodward–Hoffmann symmetry rules. The ability to attach aromatic systems to the silicon surface in a highly selective way using cycloaddition chemistry suggests that it may be possible to attach more extensively conjugated systems to silicon and other Group IV semiconductor surfaces by taking advantage of this selectivity toward an external vinyl group.

**Acknowledgment.** The authors thank Professor Charles P. Casey for a careful reading of this manuscript and many helpful suggestions. The authors also thank Dr. Dan Sykes for his assistance with the liquid-phase spectra. The authors acknowledge support from National Science Foundation Grant DMR-9901293 and the U.S. Office of Naval Research. R.J.H. and M.P.S. also thank the S.C. Johnson Co. Distinguished Fellowship program for support.

JA000928R